

Chapter 2

The Depolarisation Behaviour of Surface-Enhanced Raman Scattering Photons in a Metal Nanodimer Structure

2.1 Introduction

The metal–molecule interface provides highly attractive fields that interact with each other, such as in charge transfer. However, little is known about the materials localised at the interface. Polarised Raman measurement represents an attractive research field related to metal surfaces. The polarised SERS signal has a highly polarised character because of the anisotropic EM feature on the metal surface. Moreover, such signals are considered to have high sensitivity to the electronic state at the interface. Polarised SERS measurements give information about both the incident and Raman scattering polarisations, and several interesting polarised SERS studies have been carried out [1–13]. If one assumes a symmetrical single nanodimer structure in which only the localised EM field at the gap contributes to the enhancement, SERS depolarisation is not observed because the polarisations for excitation and scattering are the same.

Linearly polarised scattered light was observed in a metal nanodimer system by Haran et al., who reported that an asymmetric metal nanoparticle trimer generates elliptically polarised scattered light; thus, these researchers showed that the polarisation of light scattered from molecules can be manipulated on the nanometre scale [7]. A well-accepted model of the twofold EM enhancement theory for excitation and scattering for the SERS process cannot explain the present observations, because the theory predicts that the polarisation of the scattering photons is controlled in the same manner as that of the localised field [3, 14]. In contrast, depolarisation behaviour has been also reported. Polarisation rotation induced by the plasmon resonance of the SERS signal with respect to the incident polarisation was shown in arrays of uniform Au nanostructures [11]. By using an elliptic nanostructure that exhibits two LSP resonances each associated with one of the two principle axes, it was found that scattered light is resonant with another axis to one axis of the excitation process.

In the present study, the polarisation dependence on SERS from a well-ordered Ag dimer array [15] was measured in an aqueous solution containing the target molecule, 4,4'-bipyridine. In this chapter, the polarisation dependence of the scattering photons is discussed with respect to the optical properties of the metal nanostructure and adsorption structure of the target molecule.

2.2 Experimental

The Ag dimer arrays were prepared via an angle-resolved nanosphere lithography (AR-NSL) technique using repeated vapour depositions onto a polystyrene (PS)-particle (Polysciences Inc.; diameter = 350 nm) monolayer prepared on a glass substrate [16]. Aqueous PS particle suspension was concentrated to 10 wt% and then diluted by ethanol (50%). As well as the previously documented drop-coating method, I adapted another method using PS monolayers prepared on liquid–gas interfaces to improve the quality of the array. The PS solutions (20 μL) were dropped on the convex surface of a watch glass immersed in Milli-Q water. The thin water layer on the glass surface led to uniform spreading of PS beads on the air–water interface. After the spreading of PS beads on the water surface, the layer was packed tight in the course of nature. The change in the surface tension of the water around the PS layer resulted in the formation of well-ordered monolayers with a low density of defects, dislocations and vacancies on the liquid–water interface. The prepared high-quality monolayer was then lifted off the water surface using a clean glass substrate. The metal was deposited onto the PS monolayer prepared on the glass substrate. After the first metal deposition, the second metal was deposited at different angles. Then, the PS mask was removed by sonication in Milli-Q water for 10–30 s. The extinction spectrum of the metal dimer array in the visible-near infrared (NIR) region was recorded utilising a multichannel spectrometer (MCPD-2000, Ohtsuka Electronics). The structure of the dimer on the glass substrate was inspected using an atomic force microscope (AFM, Nanoscope-IIIa, Digital Instruments) in air.

A homemade polarised Raman microprobe spectrometer was specially modified for NIR laser light ($\lambda_{\text{ex}} = 785 \text{ nm}$). Raman measurements were carried out using the backscattering configuration by simultaneously collecting the scattering photons with parallel and perpendicular polarisation directions (Fig. 2.1a). The expanded NIR beam was focussed onto the sample using a water-immersion objective lens with 100 \times magnification and a numerical aperture of 1.0. The estimated spot size of irradiation of 1 μm with tunable output intensity was in the range of 10 μW –20 mW. All Raman measurements were carried out in situ via immersion of the SERS active substrates into aqueous solutions containing target molecules (4,4'-bipyridine; reagent grade, Wako Co. Ltd.) with controlled concentrations (1 μM –1 mM). The measurement on a single crystal was carried out in air by controlling the excitation polarisation direction to the crystal axis determined by XRD.

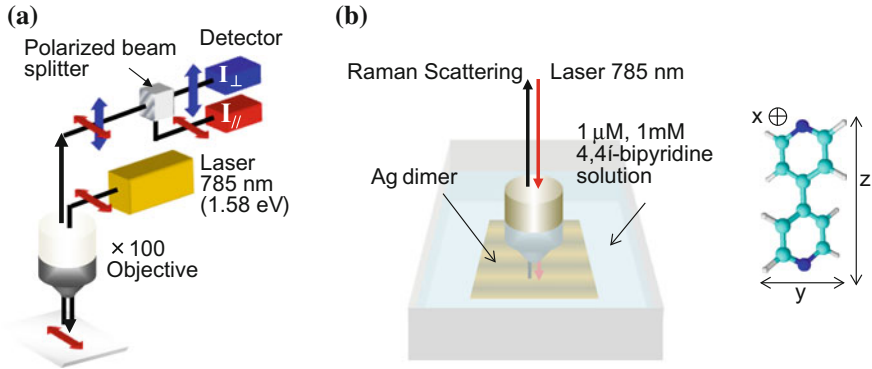


Fig. 2.1 Raman measurement configuration **a** in situ Raman cell and **b** 4,4'-bipyridine molecular structure

The stability of the metal structure was verified through polarised Rayleigh scattering light measurement. The identical polarised properties were obtained before and after light irradiation, indicating that the metal dimer structure is stable regardless of the light irradiation.

Density functional theory (DFT) calculations were carried out using the Gaussian 03, revision E.01, at the B3LYP level of DFT with 6-31G** basis sets. Calculations were carried out without the contribution of the resonance of 4,4'-bipyridine molecules. The Raman intensity was estimated as follows:

$$I \propto v_s^4 (e_s \alpha e_i)^2, \quad (2.1)$$

where v_s is the wavenumber of the Raman scattering, e_s and e_i are the unit vector along the scattering and incident electric field and α is the polarisation tensor.

2.3 Results and Discussion

For Raman band assignments, conventional polarised Raman measurements were carried out using a 15 mM aqueous solution of 4,4'-bipyridine and tetrachloromethane solution ($I_{\text{ex}} = 20 \text{ mW}$, $t_{\text{ex}} = 100 \text{ s}$). The Raman spectrum of an aqueous solution for the parallel scattering configuration showed intense peaks at 1010 and 1298 cm^{-1} and weak peaks at 764, 873 and 1229 cm^{-1} (Fig. 2.2a). For the perpendicular configuration, scattering was not clearly observed (Fig. 2.2b). This indicates that the peaks assigned to the totally symmetric modes of 4,4'-bipyridine molecules [15, 17–19] had a zero depolarisation ratio for aqueous solution. The polarised Raman spectra of tetrachloromethane solution are shown in Fig. 2.2c, d. The Raman spectrum of the tetrachloromethane solution for the parallel scattering configuration showed intense peaks at 218 (E), 314 (T_2) and

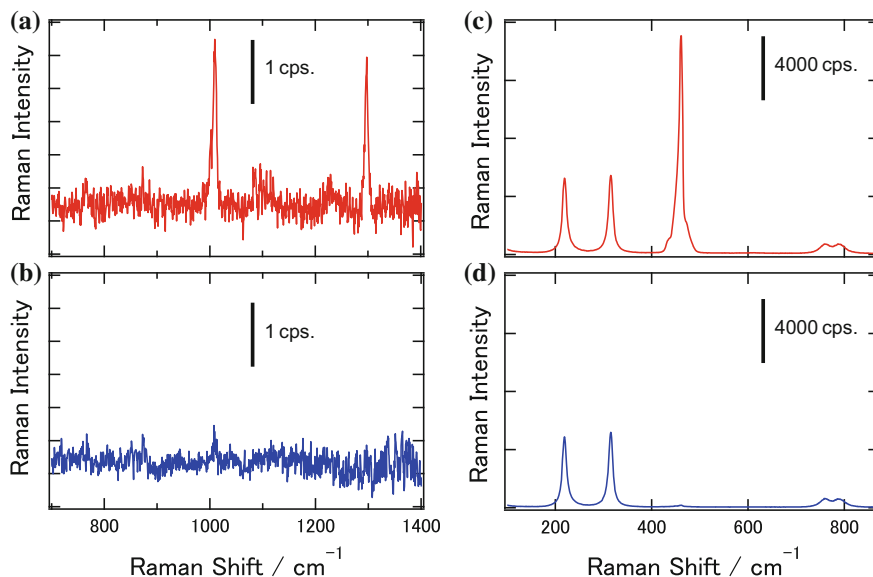


Fig. 2.2 **a, b** Polarised Raman spectrum in 4,4'-bipyridine solution and **c, d** tetrachloromethane solution: **a, c** parallel configuration and **b, d** perpendicular polarisation

460 cm^{-1} (A). Parallel scattering polarisation, which has a three-fourth depolarisation ratio for nontotally symmetric modes [218 (E) , $314\text{ cm}^{-1}\text{ (T}_2\text{)}$] with linearly polarised incident light were measured.

To investigate the Raman polarised tensor, I fabricated a single 4,4'-bipyridine crystal (Fig. 2.3a). XRD analyses showed the P_{21} symmetry in Fig. 2.3b, which is a similar symmetry to that reported previously [20]. I measured each polarisation configuration to the single crystal axis of 4,4'-bipyridine and compared this to the DFT calculation. Figure 2.3c shows the polarised Raman spectra of each polarisation configuration ($I_{\text{ex}} = 20\text{ mW}$, $t_{\text{ex}} = 10\text{ s}$). For parallel polarisation configuration on a -excitation (excitation polarisation parallel to the a -axis of a single crystal) and a -scattering (scattering polarisation parallel to the a -axis) direction, relatively strong peaks at 762 , 1000 and 1301 cm^{-1} and weak peaks at 880 , 1075 and 1230 cm^{-1} were observed. For the other parallel configurations on (b, b) and (c, c) , the same peaks were observed and the intensity ratios of the peaks were changed. The (b, b) configuration had the maximum peak intensity at 1240 cm^{-1} . In contrast, the (c, c) configuration had the maximum peak intensity at 1000 and 1300 cm^{-1} . For the perpendicular polarisation configuration on (a, b) , additional peaks at 862 , 1042 , 1215 and 1325 cm^{-1} were observed. The polarisation dependence of the intensity ratio for the parallel polarisation and appearance of additional peaks for the perpendicular polarisation were well reflected in the calculated polarised Raman spectra (Fig. 2.3d). The perpendicular configurations were

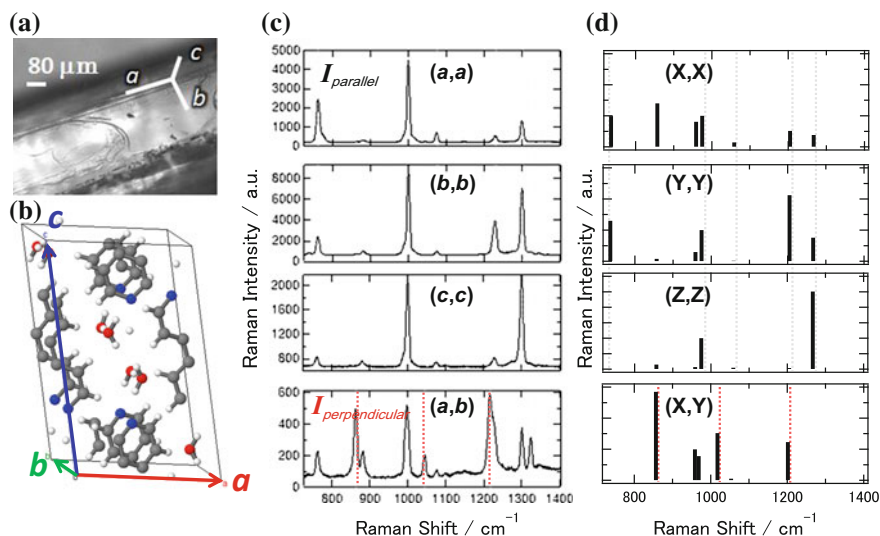


Fig. 2.3 **a** Photograph of a single 4,4'-bipyridine crystal, **b** crystal axis of the single 4,4'-bipyridine crystal, **c** polarised Raman spectrum of the single crystal in the parallel configuration and perpendicular configuration. The incident and scattering polarisation axes are shown with the notation (incident polarisation, scattering polarisation). **d** Calculated polarised Raman spectrum for parallel and perpendicular polarisation

assigned to totally symmetric a modes and the nontotally symmetric $b1$ modes of 4,4'-bipyridine molecules, respectively [15, 17–19].

The polarisation dependence on SERS was measured using the substrate with an Ag dimer array (Fig. 2.4a). The thickness and distance of the dimer structure were optimised to provide an extinction peak at around 780 nm at the parallel polarisation along the long dimer axis (Fig. 2.4b) for the excitation of the Raman measurement ($I_{ex} = 785$ nm). The dimer structure consisted of the different size Ag triangle, with a size is 50, 100 nm at each side of triangle and a height of 25, 30 nm. The gap sizes were estimated through comparison of the calculation [21]. From the extinction spectra at Fig. 2.4b, it can be observed that the polarised excitation along the long axis led to the appearance of a peak at a longer wavelength (around 800 nm). This agrees well with the theoretically calculated spectra of 'tip-to-side' Ag triangular dimers with distances of a few nanometres. Thus, the AR-NSL dimers had a gap distance of a few nanometres. The spot size irradiated to the substrate was estimated at ~ 1 μm, and this area included about 9–10 dimers. Immersed in aqueous solution containing 1 mM 4,4'-bipyridine, this substrate showed an intense SERS [15]. Polarised SERS measurements on the Ag dimmers at excitation parallel to the dimer axis exhibited well-defined polarisation behaviour (Fig. 2.4c, d). The SERS spectrum at the parallel polarisation configuration with excitation along the long dimer axis showed intense SERS peaks at 770, 871, 1016, 1074, 1231 and 1296 cm^{-1} (Fig. 2.4c). The observed SERS peaks at the parallel polarisation

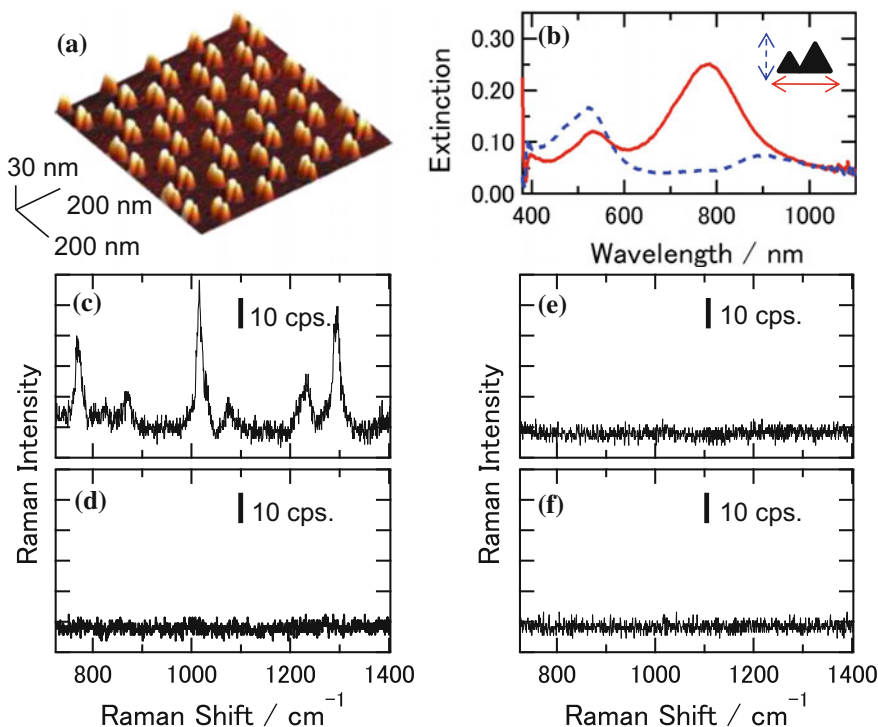
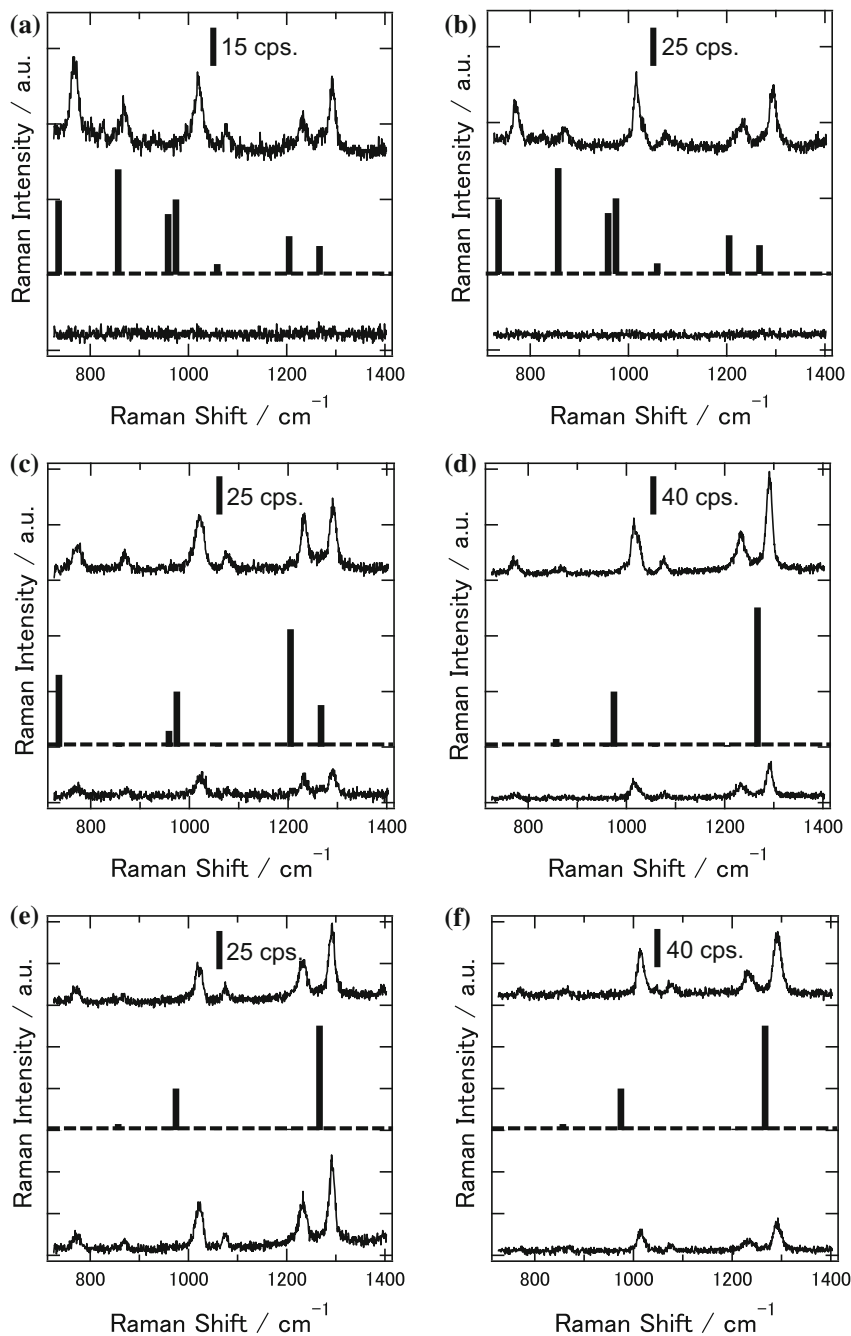


Fig. 2.4 **a** Atomic force microscope (AFM) image, **b** polarised extinction spectrum of Ag nanodimer array and SERS spectra observed in a 1 mM 4,4'-bipyridine aqueous solution at **c** parallel and **d** perpendicular polarisation configurations with parallel excitation to the dimer axis and **e** parallel and **f** perpendicular configurations with perpendicular excitation to the dimer axis ($I_{\text{ex}} = 10 \text{ mW}$, $t_{\text{ex}} = 1 \text{ s}$)

configuration could be assigned to the totally symmetric *a* modes of 4,4'-bipyridine. These peaks were not observed for the measurement on the scattering at the perpendicular configuration to the long dimer axis (Fig. 2.4d). At the perpendicular excitation to the dimer axis, scattering was not observed in either the parallel or the perpendicular configuration (Fig. 2.4e, f).

This apparent difference between the polarisation directions at the excitation demonstrated the contribution of the localised EM field at the gap of the dimers. The present system showed unique behaviour in which the polarisation of the scattering was dependent on the SERS active site and the concentration of the solution. Figure 2.5 depicts polarised SERS spectra observed in 1 mM and 1 mM 4,4'-bipyridine solutions at distinct SERS active sites under excitation parallel to the long dimer axis. At site A, perpendicular polarised scattering was not observed, as in the case shown in Fig. 2.4. Increasing the concentration to 1 mM at the same site still resulted in no perpendicular scattering (Fig. 2.5b). At site B, relatively weak perpendicular scattering was observed both in 1 μM and 1 mM solutions (Fig. 2.5c, d).



◀**Fig. 2.5** SERS spectra observed in **a, c, e** 1 mM and **b, d, f** 1 mM 4,4'-bipyridine aqueous solutions observed at **a, b** site A, **c, d** site B and **e, f** site C in the parallel (*upper*) and perpendicular (*lower*) polarisation configurations with excitation parallel to the dimer axis ($I_{\text{ex}} = 10$ mW, $t_{\text{ex}} = 1$ s); DFT calculation (*middle*) for polarisation of **a, b** X-excitation and X-scattering, **c, d** Y-excitation and Y-scattering and **d, e, f** Z-excitation and Z-scattering directions

The perpendicular scattering became much more apparent at site C (Fig. 2.5e, f). For the 1 mM solution (Fig. 2.5e), perpendicular polarised scattering was observed with comparable intensity to the parallel polarisation. For the 1 mM solution (Fig. 2.5f), perpendicular polarised scattering was weak, as in the case of site B. It should be noted that all of the observations in Fig. 2.5 were carried out before and after the confirmation that no SERS signal was observed with the excitation of perpendicular polarisation to the long dimer axis at the same site. Spectral features were also dependent on the orientation. Differences in the relative intensities between the bands and the wavenumbers should reflect the orientation of molecules relative to the localised EM field at the gap part of the dimer. Anisotropy of the highly localised EM field at the gap leads to a sensitive response in the intensity of the SERS band [22–24].

To discuss the orientation of molecules on the surface, spectral features were compared with those predicted by DFT calculation. SERS spectra at site A exhibited relatively intense bands at 770 and 871 cm^{-1} assigned to the out-of-plane ring and C–H deformation modes, respectively. These features were reproduced in DFT calculations for the polarisation in the X-direction for both excitation and scattering (middle of Fig. 2.5a, b).

The relatively strong out-of-plane modes versus the in-plane modes could be attributed to the ‘flat’ adsorption of 4,4'-bipyridine rings on the Ag surface.

A localised EM field perpendicular to the bipyridine rings on the surface may enhance the relative intensity of the band. At site B, the SERS spectrum observed at 1 mM showed a sharp increase in the relative intensity of the band at 1240 cm^{-1} (Fig. 2.5c). At 1 mM, evolution of the band at 1296 cm^{-1} was observed (Fig. 2.5d). The DFT calculations suggested that the band at 1240 cm^{-1} assigned to the in-plane C–H bending mode becomes intense with the ‘flat’ adsorption, in which the Y-axis of the molecule is normal to the metal surface. An intense band observed at 1300 cm^{-1} assigned to the interring stretching mode could be attributed to the ‘standing’ adsorption in which the molecular Z-axis is normal to the surface. The features at site C were comparable to those of site B in 1 mM solutions. The present band analysis proves the site dependence of the molecular orientation in the present system.

The relative intensities of the perpendicular to the parallel scattering in site C of Fig. 2.5 were plotted as a function of the 4,4'-bipyridine solution concentration in Fig. 2.6. Perpendicular scattering was observed, that is highly depolarised behaviour on SERS, especially at a low concentration. Depolarisation was observed when the spectral features corresponded to the ‘flat’ adsorption. To evaluate the orientation effect, we plotted the relative intensity against the Raman intensity ratios of $I_{780\text{ cm}^{-1}}/I_{1000\text{ cm}^{-1}}$ and $I_{1300\text{ cm}^{-1}}/I_{1000\text{ cm}^{-1}}$ in Fig. 2.7. As shown in the DFT

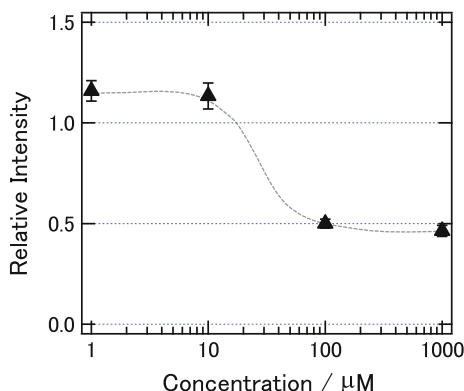


Fig. 2.6 Relative SERS intensity ratio of the perpendicular and parallel polarisation configurations with parallel excitation to the dimer axis at various 4,4'-bipyridine concentrations (site C)

calculation, the 'flat' adsorption of 4,4'-bipyridine rings on the Ag surface indicated an intense band at 780 cm^{-1} , and the 'standing' adsorption—in which the Y-axis of the molecule is normal to the metal surface—indicated an intense band at 1300 cm^{-1} . These correlations illustrate that the intense $I_{780\text{ cm}^{-1}}/I_{1000\text{ cm}^{-1}}$ corresponds to the 'flat' adsorption, and the intense $I_{1300\text{ cm}^{-1}}/I_{1000\text{ cm}^{-1}}$ corresponds to the 'standing' adsorption. 'Flat' adsorption tends towards low relative intensity in Fig. 2.7a. In contrast, 'standing' adsorption indicates high relative intensity in Fig. 2.7b. The present observation of the depolarisation behaviour clearly demonstrated that the orientation of molecules at the gap affected the polarisation of the scattering process. The polarised dependence of SERS has been discussed with

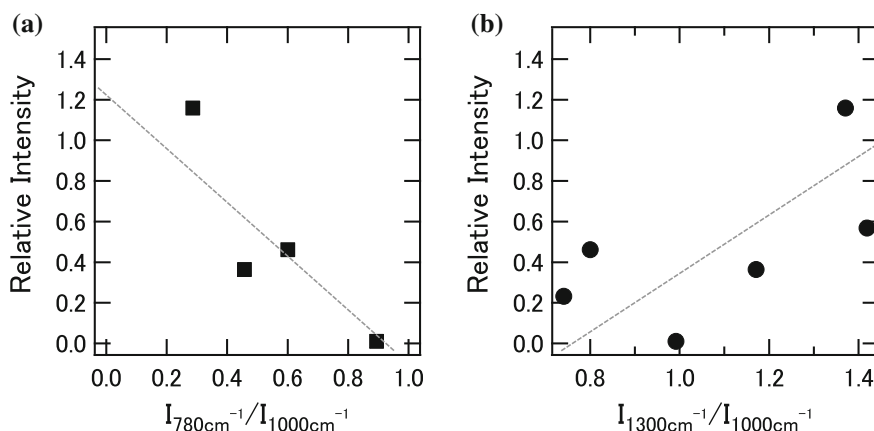


Fig. 2.7 Relative intensity ratio of the parallel and perpendicular polarisation configurations with parallel excitation to the dimer axis at Raman intensity ratios of $I_{780\text{ cm}^{-1}}/I_{1000\text{ cm}^{-1}}$ and $I_{1300\text{ cm}^{-1}}/I_{1000\text{ cm}^{-1}}$; all concentrations are $1\text{ }\mu\text{M}$

respect to the individual tensors for the excitation field and the scattering field [7, 11]. To explain the present observation concerning the depolarisation of the scattering photons, selective contributions to the scattering process should be considered. One of the possible contributions is the two different resonance modes of LSPR, which respectively relate to incident and scattering polarisation. The extinction of the Ag dimer at a longer wavelength region >850 nm in perpendicular polarisation contributes to the resonance of the Raman scattering at perpendicular polarisation around 1300 cm^{-1} (874 nm). This perpendicular polarisation, as well as the nondiagonal terms in the polarisability tensor that depend on the orientation of adsorbed molecules, could induce the perpendicular scattering. This process, however, is not adequate to explain the present observation because of relatively small intensities of the extinction of the metal structure and the nontotally symmetric bands of a single crystal. Another possibility is that the scattering depolarisation observed in the present system could be induced by the resonance of the scattering photons with the localised electronic states caused by the specific adsorption. In the present system, 4,4'-bipyridine molecules adsorbed on the metal surface tended to have the 'standing' structure when the concentration was more than a few tens of mM due to the coordination ability of the nitrogen atom and the intermolecular interaction [25, 26]. Specific adsorption of molecules could lead to the formation of localised electronic states at the molecule and metal interface. The contribution of the localised resonance states to the SERS process has been considered as an excitation process involving the CT contribution, the so-called chemical effect, leading to the observation of nontotally symmetric modes [26]. Although the observed bands in the SERS spectra in the present system were fully assigned to totally symmetric modes, characteristics of the SERS spectral features, such as relatively intense bands at 1229 and 1298 cm^{-1} compared with those in bulk solution and a single crystal, could imply a CT contribution [17]. To demonstrate the contribution of the resonance of the localised states to the depolarisation, further detailed analysis is required using a system showing well-controlled single-molecule SERS.

2.4 Conclusion

In conclusion, the substrate with a Ag nanodimer array immersed in 4,4'-bipyridine solution showed depolarised SERS behaviour depending on the adsorbed structure of molecules at the dimer's gaps. The orientation of molecules was discussed by comparing SERS spectra with those obtained from conventional polarised Raman spectra of a homogeneous aqueous solution and a single crystal of 4,4'-bipyridine. The SERS depolarisation at specific adsorption states of molecules implies that the molecule and metal interface modulate the scattering polarisation selectively.

References

1. M. Moskovits, J.S. Suh, *J. Phys. Chem.* **88**, 1293–1298 (1984)
2. H. Sano, G. Mizutani, S. Ushioda, *Phys. Rev. B* **47**, 13773–13781 (1993)
3. K.A. Bosnick, Jiang, L.E. Brus, *J. Phys. Chem. B* **106**, 8096–8099 (2002)
4. Jiang, K. Bosnick, M. Maillard, L. Brus, *J. Phys. Chem. B* **107**, 9964–9972 (2003)
5. H. Xu, M. Kall, *ChemPhysChem* **4**, 1001–1005 (2003)
6. T.O. Shegai, G. Haran, *J. Phys. Chem. B* **110**, 2459–2461 (2006)
7. T. Shegai, Z. Li, T. Dadosh, Z. Zhang, H. Xu, G. Haran, *Proc. Natl. Acad. Sci. U.S.A.* **105**, 16448–16453 (2008)
8. Z. Li, T. Shegai, G. Haran, H. Xu, *ACS Nano* **3**, 637–642 (2009)
9. E.C. Le Ru, P.G. Etchegoin, *Chem. Phys. Lett.* **423**, 63–66 (2006)
10. E.C. Le Ru, M. Meyer, E. Blackie, P.G. Etchegoin, *J. Raman Spectrosc.* **39**, 1127–1134 (2008)
11. E.C. Le Ru, J. Grand, N. Félidj, J. Aubard, G. Lévi, A. Hohenau, J.R. Krenn, E. Blackie, P.G. Etchegoin, *J. Phys. Chem. C* **112**, 8117–8121 (2008)
12. A. Moroz, *J. Opt. Soc. Am. B* **26**, 517–527 (2009)
13. K.D. Jernshøj, S. Hassing, *J. Raman Spectrosc.* **41**, 727–738 (2010)
14. K.-I. Yoshida, T. Itoh, V. Biju, M. Ishikawa, Y. Ozaki, *Phys. Rev. B* **79**, 085419 (2009)
15. Y. Sawai, B. Takimoto, H. Nabika, K. Ajito, K. Murakoshi, *J. Am. Chem. Soc.* **129**, 1658–1662 (2007)
16. U.C. Fischer, H.P. Zingsheim, *J. Vac. Sci. Tech.* **19**, 881–885 (1981)
17. J.K. Lim, S.-W. Joo, *Surf. Interface Anal.* **39**, 684–690 (2007)
18. A. Topaçlı, S. Akyüz, *Spectrochim. Acta Part A Mol. Biomol. Spectrosc.* **51**, 633–641 (1995)
19. A.L. Kamysny, V.N. Zakharov, Y.V. Fedorov, A.E. Galashin, L.A.J. Aslanov, *Colloid Interface Sci.* **158**, 171–182 (1993)
20. C. Näther, J. Riedel, I. Jeß, *Acta Crystallogr. Sect. C* **57**, 111–112 (2001)
21. E. Hao, G.C. Schatz, *J. Chem. Phys.* **120**, 357–366 (2004)
22. D. Battisti, R. Aroca, R.O. Loutfy, *Chem. Mat.* **1**, 124–128 (1989)
23. P.G. Gucciardi, F. Bonaccorso, M. Lopes, L. Billot, M.L. de la Chapelle, *Thin Solid Films* **516**, 8064–8072 (2008)
24. K. Uosaki, H. Allen, O. Hill, *J. Electroanal. Chem. Interfacial Electrochem.* **122**, 321–326 (1981)
25. D. Yang, D. Bizzotto, J. Lipkowski, B. Pettinger, S. Mirwald, *J. Phys. Chem.* **98**, 7083–7089 (1994)
26. J.R. Lombardi, R.L. Birke, *Acc. Chem. Res.* **42**, 734–742 (2009)

Studies on the Plasmon-Induced Photoexcitation
Processes of Molecules on Metal Surfaces

Nagasawa, F.

2017, XII, 77 p. 40 illus., 36 illus. in color., Hardcover

ISBN: 978-4-431-56577-2